Collapse of itinerant ferromagnetism in CoS_2 under pressure: An x-ray absorption spectroscopy study

E. Mijit,[1,2] K. Chen,[1,*] F. Choueikani,[1] A. Di Cicco,[2] and F. Baudelet[1]
[1]*Synchrotron SOLEIL, L'Orme des Merisiers, Saint-Aubin, Boîte Postale 48, 91192 Gif-sur-Yvette Cedex, France*
[2]*Physics Division, School of Science and Technology, Università di Camerino, Via Madonna delle Carceri 9, I-62032 Camerino, Macerata, Italy*

(Received 10 July 2018; revised manuscript received 18 October 2018; published 20 November 2018; corrected 4 January 2023)

Cobalt L-edge x-ray absorption spectra (XAS) and x-ray magnetic circular dichroism (XMCD) of CoS_2 have been measured at low temperature (4 K) in order to characterize the electronic and magnetic structure with a significant improvement in resolution as compared with previous measurements. The branching ratio of L_3 and L_2 x-ray absorption near-edge spectra was found to be consistent with a low-spin configuration ($S = 1/2$). A total magnetic moment $\langle m \rangle = 0.78\,\mu_B$/Co atom with the orbital part $\langle m_l \rangle = 0.049\,\mu_B$ has been obtained from the XMCD signal, consistent with the nearly half-metallic character of CoS_2 and with the itinerant nature of the ferromagnetism. The behavior under pressure of CoS_2 was studied by Co K-edge XAS and XMCD experiments performed up to a pressure of about 30 GPa using diamond-anvil cell at a temperature of 10 K. No evidence of structural phase transition was observed, while the intensity of the XMCD signal was found to decrease continuously for increasing pressures, becoming negligible in the $8 \sim 10$ GPa pressure range, a fact consistent with the collapse of itinerant ferromagnetic ordering. The gradual change in the electronic and magnetic structure upon application of pressure was also monitored by the near-edge XAS evolution, found to be in agreement with full multiple-scattering calculations under uniform contraction of distances, and by the blue-shift of the K-edge energy. The Co K-edge energy was found to shift to higher energies (up to 0.64 eV at 30 GPa) and a change of slope was observed at pressures around 5 GPa that may correspond to the disappearance of half-metallicity, in agreement with previous studies.

DOI: 10.1103/PhysRevB.98.184423

I. INTRODUCTION

The cubic pyrite-type compound cobalt disulphide (CoS_2) is a metallic paramagnet at room temperature which experiences a continuous phase transition to the ferromagnetic state at $T_c = 122$ K [1,2], accompanied by an increase of resistivity [3]. In CoS_2, divalent Co^{2+} ions are located at the center of octahedrons formed by S_2^{2-} dimers [4]. The strong octahedral field splits the $3d$ band of Co ions into t_{2g} and e_g subbands with the low-spin configuration of $t_{2g}^6 e_g^1$, thus half-metallic (HM) character with high- or full-spin polarization (which might be exploited in spin-dependent electronic devices) was expected. The interesting electronic and magnetic behavior of CoS_2 attracted considerable attention over the years; however, different theoretical and experimental studies gave controversial results on its half-metallicity, the amount of electron correlations, or the nature of the magnetism.

Most of the first-principle calculations favored the nearly half-metallic ground state or the half-metallic ground state, except for the normal metallic electronic structure obtained by Yamada *et al.* using the linear muffin-tin orbital (LMTO) method with the atomic sphere approximation [5]. Zhao *et al.* have found CoS_2 is almost half-metallic in the sense that the number of the occupied minority spin states in the $e_{g\downarrow}$ band is quite small compare to that of the majority spin states in the $e_{g\uparrow}$ band [6]. Shishidou *et al.* were able to obtain a half-metallic character of CoS_2 by using the full-potential linearized augmented plane-wave method combined with the generalized gradient approximation for the exchange-correlation potential [7]. Kwon *et al.* investigated the electronic structure of CoS_2 using the local spin-density approximation (LSDA) and taking into account the effect of the Coulomb correlation by the LSDA + U method [8]. They also obtained the ferromagnetic ground state with the nearly half-metallic nature. The Coulomb correlation at Co sites was limited, thus CoS_2 was categorized as an itinerant ferromagnet. Experimentally, the measured saturation magnetic moment of $0.84\mu_B$/Co in the ferromagnetic state is close to, but not equal to, the value expected for $S = 1/2$ [2]. The point contact Andreev reflection measurement on the polycrystalline CoS_2 shows a low-spin polarization of 56% [9], indicating CoS_2 is not a half metal. Polarized neutron diffraction experiments also shows that the half-metallic character is not observed in the ferromagnetic phase [10]. The reflectivity study of Yamamoto *et al.* proposed the half-metallicity with a totally unoccupied Co $e_{g\downarrow}$ band (in spin-down channel) located above the Fermi level [11]. Contrary to this, high-resolution photoemission spectroscopy suggested a partially filled Co $e_{g\uparrow}$ band, consistent with the relatively small saturation magnetic moment [12]. Temperature dependencies of the electrical resistivity as well as the small magnetic entropy were described well by the itinerant electron model [13–15]. However, polarized neutron diffraction results showed dominant magnetic

*kaichen.hzg@gmail.com

moment localization around Co nuclei, and preferred the localized electron picture with strong electron correlation [16]. Features of the later dynamical susceptibility measurements by inelastic neutron scattering evidenced the itinerant nature of the ferromagnetism in CoS_2 [17].

Effects of external and chemical (by doping of Se or other elements) pressures were investigated by means of resistivity and magnetic susceptibility measurements. Both effects reduced T_c and made the magnetic phase transition first order [18–22]. The magnetic ordering temperature was tuned to zero by external pressure at 4.8 GPa, indicating the existence of a first-order quantum phase transition [21,22].

In the present study, we measured x-ray adsorption spectra (XAS) and x-ray magnetic circular dichroism (XMCD) signals at the Co L edges ($T = 4$ K, $\mu_0 H = 6.5$ T) of CoS_2 under improved conditions of energy resolutions with respect to previous investigations. The measurements were carried out to verify previous debated hypothesis about the nature of ferromagnetism and the half-metallic state of CoS_2 with a low-spin configuration of Co^{2+}. Combined Co K-edge XAS and XMCD experiments under high pressure were carried out, assisted by advanced multiple-scattering simulations, with the aim of studying the interplay between structural, electronic, and magnetic properties for increasing pressures.

II. EXPERIMENTS AND SIMULATIONS

The Co L-edge XAS and XMCD spectra at $T = 4$ K have been collected at the DEIMOS beamline [23] of Synchrotron SOLEIL, using circular left- and right-polarized x rays, under high magnetic field of $\mu_0 H = 6.5$ T. CoS_2 powders from Alfa Aesar (No. 14005 cobalt sulfide) were compressed into a pellet for XAS data collection using the total electron yield mode. Pressure-dependent Co K-edge XAS and XMCD measurements have been performed at low temperature (10 K) using the transmission mode in the ODE beamline of Synchrotron SOLEIL [24]. CoS_2 powders have been loaded into the 125-μm-diameter hole of a rhenium gasket with silicon oil as the pressure medium and subjected to high pressure up to 30 GPa in a membrane diamond-anvil cell. Pressure was calibrated in a standard way measuring the ruby fluorescence line shift. XAS were collected at the Co K-edge (~7723 eV) with a fixed circular polarized helicity with magnetic field $H = 0$, while the XMCD was obtained through the modification of XAS measured under a magnetic field of $\mu_0 H = 1.3$ T applied parallel or antiparallel to the beam helicity.

Two sets of *ab initio* full multiple scattering (FMS) calculations were performed using the XMAN code [25] to better understand the pressure response of Co K-edge XAS. First of all, based on the reported pyrite structure [4] under ambient conditions, we carried out calculations using increasing cluster sizes (7, 15, 27, 33, 51, 57, and 71 atoms) to check the scattering contributions from the consecutive S and Co shells surrounding the absorbing atom. The second set of calculations was done for several clusters (with equal number of 125 atoms) generated by reducing (2%–12%) the ambient-pressure lattice constant [4] a = 5.5385 Å in order to simulate the effect of uniform lattice compressions under pressure (10% lattice contraction here approximately corresponds to a pressure of 45 GPa, by a simple linear extrapolation of the pressure volume relation in Ref [26]). FMS calculations were carried out using muffin-tin optical potentials, including a real Hedin-Lundqvist exchange-correlation term, and broadening the calculated spectrum with an energy-dependent Lorentzian function to take into account the core hole lifetime, experimental resolution, and inelastic processes. The excited configuration of the photoabsorber was used to simulate the charge relaxation around the core hole.

III. RESULTS AND DISCUSSION

A. Co L-edge XAS and XMCD

XMCD is a very powerful probe of magnetic properties thanks to its element and site specificity and its ability to separate the spin and orbital contributions to the magnetic moment. The Co L-edge XAS with circular right (σ^+)- and left (σ^-)-polarized x rays and XMCD (σ^+-σ^-) spectra are shown in Fig. 1(a). Our Co L-edge XAS have more clear multiplet features compare to the old measurements [27,28] thanks to the increasing spectral resolutions in synchrotron facilities over the years. With the fully occupied t_{2g} orbitals in CoS_2, the L_2- and L_3-edge transitions originate from the $2p_{1/2}$ and $2p_{3/2}$ core states to the Co $3d$ bands with e_g symmetry, respectively. The features at $6 \sim 8$ eV higher energies of L_3 and L_2 edges are due to the transitions to the unoccupied Co $4s$ conduction bands, according to the calculated density of states in the corresponding energy region above the Fermi level [29]. In Fig. 1(b), the Co L-edge XAS ($\sigma^+/2 + \sigma^-/2$) of CoS_2 is compared with the L-edge spectrum of CoO, which is characterized by a high-spin state of Co^{2+} ($t_{2g}^5 e_g^2$, $S = 3/2$). As expected, peak positions coincide while XAS show different profiles indicating the same valence (Co^{2+}) in CoS_2 with a different low-spin state ($t_{2g}^6 e_g^1$, $S = 1/2$). The spin state also can be identified by the branching ratio which is defined as $B_{\mathrm{BR}} = C_{L_3}/(C_{L_3} + C_{L_2})$, where C_L values are the integrals of the corresponding L-edge absorption spectra. In fact, it is known that high-spin states show $2p$ branching ratios higher than those of low-spin states [30]. As shown in Fig. 1(c), those integrals are $C_{L_3} = 11.22$ and $C_{L_2} = 3.8$, respectively, resulting in a branching ratio of $B_{\mathrm{BR}} \sim 0.75$ in CoS_2. This value can be compared with that of CoO ($B_{\mathrm{BR}} = 0.83$), consistent with the assignment of a low-spin state of Co^{2+} in CoS_2.

Typical positive-negative magnetic circular dichroism signals are observed in the XMCD spectra. The spin and orbital contributions of the magnetic moment can be derived from the XAS and XMCD spectra according to the magneto-optic sum rule [31]:

$$\langle m_l \rangle = -n_h \frac{2(A+B)}{3C}, \quad \langle m_s \rangle = -n_h \frac{(A-2B)}{C},$$

where $\langle m_l \rangle$ and $\langle m_s \rangle$ are spin and angular momenta in units of μ_B/atom, respectively, and n_h represents the number of $3d$ vacancies in the metal ion (which is equal to 3 in the case of Co^{2+}). The parameters $A = -1.47(5)$, $B = 1.10(5)$, and $C = 15.02(5)$ are the integrals of XMCD intensities over L_3 and L_2 edges and the total XAS integral, respectively [see Fig. 1(d)]. Using the above relations, $\langle m_s \rangle = 0.733\,\mu_B$ and $\langle m_l \rangle = 0.049\,\mu_B$ can be derived for each Co atom, with the total magnetic moment $\langle m \rangle = 0.782\,\mu_B$. This value is close to previous experimental values and slightly smaller

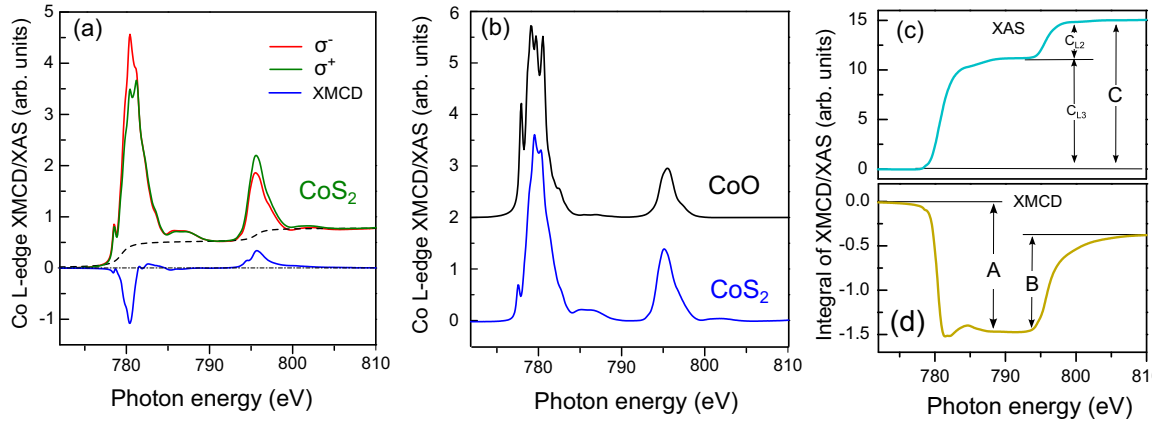

FIG. 1. (a) Co $L_{2,3}$-edge XAS for right (σ^+)- and left (σ^-)-polarized x rays and XMCD (σ^+-σ^-) spectra (lower curve). The dashed line is the L-edge jump baseline subtracted for calculating the integrals shown in panel (c). (b) Co $L_{2,3}$-edge XAS ($\sigma^+/2 + \sigma^-/2$) compared with that of CoO (upper curve), which is characterized by a high-spin state of Co^{2+}. (c) Integral of the Co $L_{2,3}$-edge XAS of CoS_2 reported in panel (b) (lower curve), with numerical results $C = 15.02(5)$, $C_{L_3} = 11.22(5)$, and $C_{L_2} = 3.80(5)$. (d) Integral of the XMCD spectrum shown in panel (a) (lower curve), $A = -1.47(5)$ and $B = 1.10(5)$.

then the expected magnetic moment ($\langle m \rangle = 1\,\mu_B$) of the perfect half-spin state and indicates the nearly half-metallic character of CoS_2. These results can be used to calculate the ratio of orbital and spin angular momenta $\langle L_z \rangle / \langle S_z \rangle = g_e * (m_l)/(m_s) = 0.133$, where $g_e = 2$ is the gyromagnetic ratio. This value is slightly smaller than those found in previous studies, e.g., 0.14 [27], 0.18 [28], and 0.15 [8], still suggesting the existence of a finite value for the orbital momentum. This may be unexpected for Co in the low-spin state with a large crystal field splitting ~2.5 eV. However, the corresponding Coulomb correlations to this non-negligible orbital magnetic moment is rather small according to LSDA + U calculations [8], so CoS_2 can be classified as an itinerant ferromagnet.

B. Co *K*-edge XAS and XMCD

The pressure-induced magnetic transition in CoS_2 was investigated by using Co K-edge XAS and XMCD spectra, probing mainly the empty states of p-like character. The sensitivity to magnetic properties for K-edge XAS originates from the spin-orbit coupling in the empty $4p$ states due to on-site and intrasite exchange interactions with polarized $3d$ states, the so called p-d hybridization [32–34]. The intensity of the K-edge XMCD spectra yields a direct measurement of the expectation value of the $4p$ orbital angular momentum, which is proportional to the magnetic moment of $3d$ states [35].

In Figs. 2 and 3, we present the normalized Co K-edge XAS and the XMCD signals of CoS_2 collected under increasing pressures up to $P = 30$ GPa. We do not show totally suppressed XMCD signals above 10 GPa in Fig. 3 for which the magnetic signal is negligible. The pre-edge peak (I) in Fig. 2 probes the Co $3d$ states hybridized with the Co $4p$ states, does not change within the experimental precision, and appears at a fixed energy (~7718 eV) in the investigated pressure range. The Co K-edge XAS can be interpreted in the framework of current one-electron dipole approximation theories. In the language of molecular orbital theory the broad white line (in the energy range of 7720 ~ 7760 eV, described by two features a and b) is generally ascribed to the empty Cobalt $4p$ states. Within the multiple-scattering theory commonly used for the interpretation of the XAS, features a, b, and c of Fig. 2 are associated with photoelectron

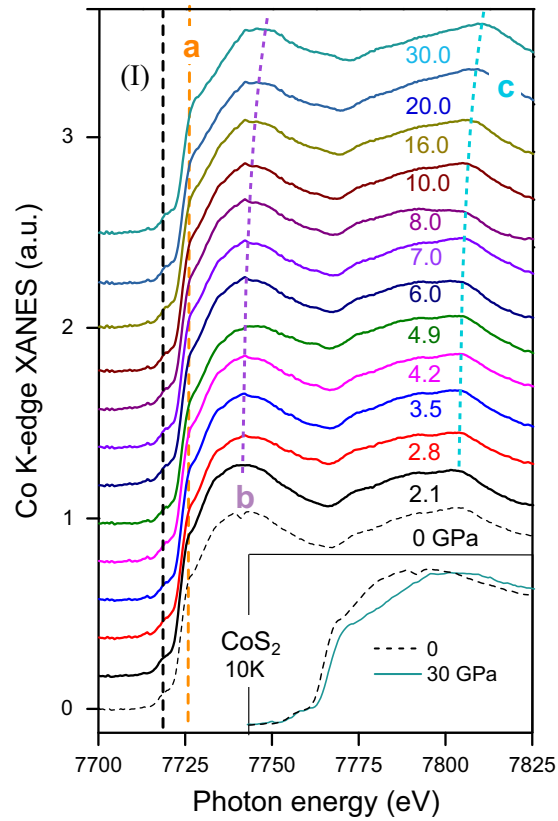

FIG. 2. Pressure-dependent Co K-edge x-ray absorption near-edge (XANES) spectra measured at 10 K in the range of 0–30 GPa. Features a, b, and c shift to slightly higher photon energies as an effect of the volume contraction. A direct comparison among the XAS at 0 and 30 GPa is reported at the bottom, showing a visible blue-shift of the absorption edge. The prepeak (I) is substantially unchanged with pressure.

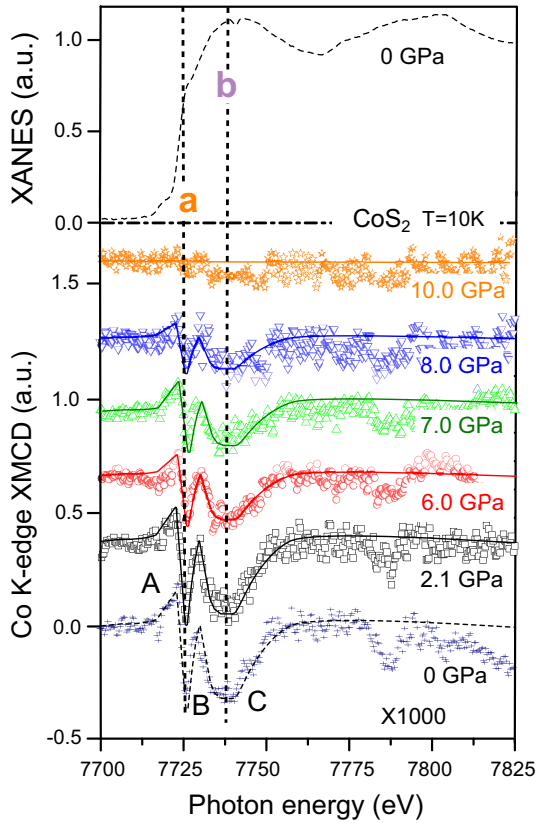

FIG. 3. Pressure-dependent XMCD spectra, characterized by clear features labeled as A, B, and C, are shown for increasing pressure from the bottom to the top. The curved lines are guides for the eye to better see the trend of the experimental data. The data of totally suppressed XMCD signal after 10 GPa are not given. The topmost XAS recorded at ambient pressure is shown for comparison.

scattering resonances within the neighboring atomic shells. As can be seen in Fig. 4(a), cluster size-dependent calculations show that we need to include at least five shells of neighbors to reproduce features a, b, and c. A cluster including the sixth shell of neighbors (57 atoms in total) is found to be necessary for convergence and final good agreement with the experimental spectra.

As can be seen in Fig. 2, there are no noticeable changes in the XAS profiles under pressure except the gradual blue-shift of features b and c to higher energies. The increased energy distance between features a and b upon compression is not related to a change of the white line profile, but mainly to the shift of the b position associated with a decrease of Co-S bonding length, following Natoli's rule [36]. The blue-shift of feature c is also due to similar effects of lattice compression. As shown in Fig. 4(b), these effects of lattice compression are nicely reproduced in our theoretical XAS for various degrees of the lattice contraction.

The pressure-dependent Co K-edge absorption threshold (E_0), determined as the maximum of the first derivative of the near-edge absorption spectra, is given in Fig. 5(a). A continuous shift of the edge energy towards higher photon energies is observed, and a change of slope is clearly observed at $P = 4 \sim 6$ GPa. The maximum energy shift observed at 30 GPa is around 0.64 eV.

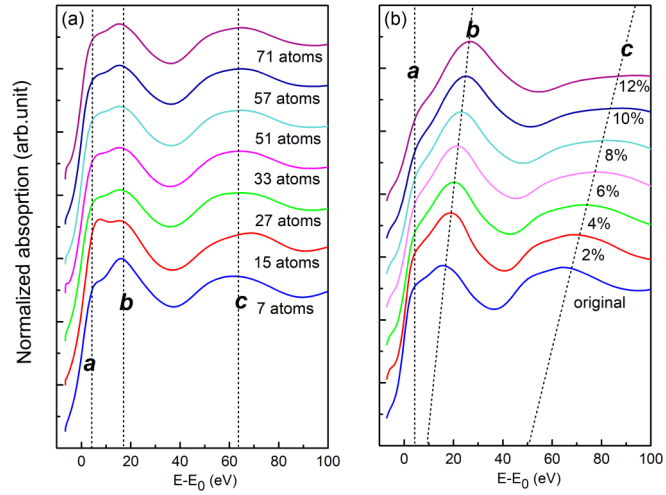

FIG. 4. Full multiple-scattering calculations of Co K-edge XAS as a function of (a) cluster size and (b) uniform lattice contraction. The theoretical spectra in panel (a) and the first spectra (labeled as original) in panel (b) were obtained using the pyrite structure under ambient conditions and correspond to the experimental spectra taken at 0 GPa. A 10% contraction corresponds roughly to an external pressure of about 45 GPa by extrapolating the pressure volume relation in Ref. [26].

As shown in Fig. 3, the K-edge XMCD spectrum of CoS_2 can be characterized by a maxima, A, and two minima, B and C. These XMCD spectra show some similarities with the features of the simulated spectra obtained by the LMTO method in a previous first-principle study [29] which also has one positive and two negative peaks. However, the position and intensity of feature C are rather different. Upon compression, the XMCD intensity shown in Fig. 5(b) decreases quickly after $3 \sim 5$ GPa and is finally quenched at 10 GPa. The fast drop of XMCD intensity around 5 GPa indicates the starting point of the collapse of ferromagnetic ordering and the transition into the paramagnetic phase.

C. Magnetic phase transition

No evidence of structural phase transitions in CoS_2 has observed for increasing pressure up to 30 GPa, and the ambient-pressure pyrite structure is preserved, as monitored by the Co K-edge experimental and calculated XAS shown in Figs. 2 and 4(b). Moreover, the pressure response of XMCD spectra does not show any sharp transition, at variance with previous studies [18–22,37]. A possible reason of this inconsistency may be due to the different experimental methods. In previous high-pressure studies, experiments were carried out under isobaric conditions, varying the temperature across the ferromagnetic-paramagnetic transition. In the present isothermal experiment, however, the loss of ferromagnetic ordering was induced by pressure. Pressure gradients may play a role, but even in the presence of a sharp ferromagnetic to paramagnetic transition, a gradual decrease of the XMCD signal can also be observed due to the parallel magnetic moments along the field applied during the measurements.

While the disappearance of the XMCD signal appears to be a continuous process for increasing pressures, it is important to remark that a change of slope in the pressure-dependent

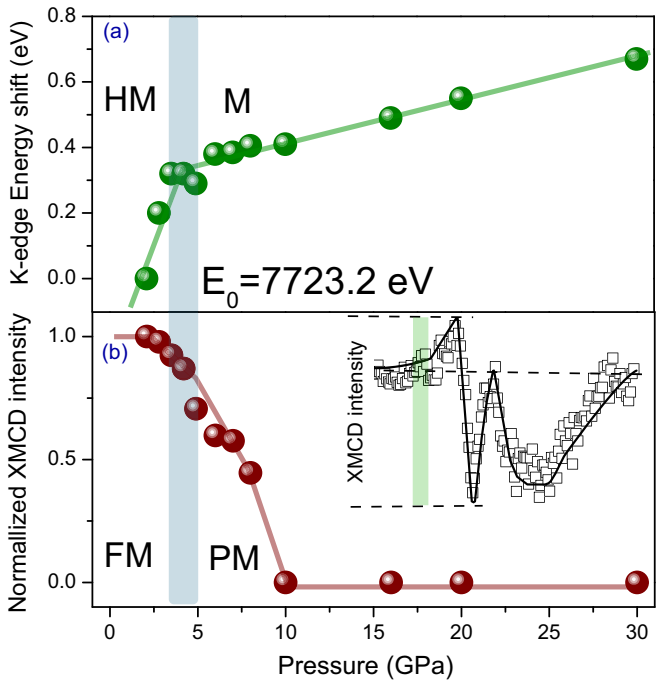

FIG. 5. (a) Pressure response of the Co K-edge energy E_0 (eV). Pressures related to the change of slope are shaded. (b) Co K-edge XMCD intensity for increasing pressure, normalized to the value at 2.1 GPa. The XMCD intensity (as shown in the inset) is defined as the height difference of positive and negative (relative to the horizontal dashed line in the middle) peaks. The shaded region can be used to identify a transition from a half-metallic (HM) state to a metallic (M) state and from a ferromagnetic (FM) state to a paramagnetic (PM) state.

edge energy shift was observed around ∼5 GPa [as shown in Fig. 5(a)], in good agreement with the critical pressures of ferromagnetic-paramagnetic transition reported by the previous isobaric experiments [21,22]. Those previous studies are also in qualitative agreement with the declining range of the XMCD intensity as shown in Fig. 5(b). As the Co^{2+} valence is unchanged with pressure, the edge shift appears to be essentially related with the volume compression, leading to a shortening of the Co-S bonding lengths. The decrease of the bonding lengths leads to an increase of the electron band energy as a result of the higher overlap of electron densities. The overlap for the $4p$ delocalized states are more significant than localized $1s$ levels, consequently the absorption edge shifts toward higher energies. This parallel behavior of the edge energy shift and the XMCD intensity suggests a strong interplay of lattice compression, changes in the electronic band structure, and magnetic ordering.

It should be noted that the pressure-induced loss of ferromagnetism in CoS_2 has been explained by Liu *et al.* [37]. According to their DFT calculations with the LMTO method, the loss of ferromagnetic ordering is due to the reduction of exchange splitting in the Co $3d$ band by external pressure, a substantial increase in the density of states (DOS) of the spin-down subband, and suppression of half-metallicity. However, in the framework of itinerant magnetism and its dependence on the band structure, the magnetic transition may also be explained by a possible change in the band width. The application of pressure induces a reduction of the interatomic distances and enhances the overlap of the atomic wave functions, eventually leading to a broadened d band and a reduced DOS in the vicinity of the Fermi level. The Stoner criterion is no longer satisfied when the DOS is small enough, resulting in a drop of the magnetic moment and instability of the ferromagnetic ordering. This interpretation is supported by previous examples of bandwidth-driven electronic transitions (insulator to metal transitions for instance) without structural phase transformation, as widely discussed in literature [38,39]. In the present case, the band overlap effect can also explain the HM to metallic transition associated with the ferromagnetic to paramagnetic transition which may be located in the vicinity of the observed change of slope as shown in Fig. 5(b).

IV. CONCLUSIONS

In this work, cobalt L-edge x-ray absorption spectra (XAS) and x-ray magnetic circular dichroism (XMCD) in CoS_2 were presented confirming the low-spin configuration of Co^{2+} with a significant improvement in energy resolution as compared with previous soft x-ray measurements. The XMCD signals have been found to be consistent with the nearly half-metallic character of CoS_2 and with the itinerant nature of the ferromagnetism. The behavior under pressure of CoS_2 was studied by combined Co K-edge XAS and XMCD experiments performed up to a pressure of about 30 GPa at a temperature of 10 K. The evolution of the XAS for increasing pressures was studied also by means of full multiple-scattering simulations. No structural phase transitions were observed, and XAS can be interpreted by a simple volume compression of the pyrite ambient-pressure structure. The intensity of the XMCD signal was found to decrease without sharp transitions for increasing pressures, becoming negligible in the $8 \sim 10$ GPa pressure range. The K-edge absorption threshold E_0 was found to shift to higher energies (up to 0.64 eV at 30 GPa) with pressure and a change of slope was observed at pressures around 5 GPa. The parallel gradual changes in the electronic and magnetic structure upon application of pressure were interpreted as a consequence of the collapse of itinerant ferromagnetic ordering and of the half-metallicity in CoS_2, in substantial agreement with previous studies.

ACKNOWLEDGMENT

We acknowledge SOLEIL for provision of synchrotron radiation facilities.

[1] M. R. Benoit, J. Chim. Phys. **52**, 119 (1955).
[2] B. Morris, V. Johnson, and A. Wold, J. Phys. Chem. Solids **28**, 1565 (1967).
[3] S. Ogawa and T. Teranishi, Phys. Lett. A **36**, 407 (1971).
[4] E. Nowack, D. Schwarzenbach, and T. Hahn, Acta Crystallogr. **47**, 650 (1991).
[5] H. Yamada, K. Terao, and M. Aoki, J. Magn. Magn. Mater. **177-181**, 607 (1998).

[6] G. L. Zhao, J. Callaway, and M. Hayashibara, Phys. Rev. B **48**, 15781 (1993).
[7] T. Shishidou, A. J. Freeman, and R. Asahi, Phys. Rev. B **64**, 180401(R) (2001).
[8] S. K. Kwon, S. J. Youn, and B. I. Min, Phys. Rev. B **62**, 357 (2000).
[9] L. Wang, T. Y. Chen, and C. Leighton, Phys. Rev. B **69**, 094412 (2004).
[10] P. J. Brown, K. U. Newmann, A. Simon, F. Ueno, and R. A. Ziebeck, J. Phys.: Condens. Matter **17**, 1583 (2005).
[11] R. Yamamoto, A. Machida, Y. Moritomo, and A. Nakamura, Phys. Rev. B **59**, R7793 (1999).
[12] T. Takahashi, Y. Naitoh, T. Sato, T. Kamiyama, K. Yamada, H. Hiraka, Y. Endoh, M. Usuda, and N. Hamada, Phys. Rev. B **63**, 094415 (2001).
[13] H. S. Jarrett, W. H. Cloud, R. J. Bouchard, S. R. Butler, C. G. Frederich, and J. L. Gillson, Phys. Rev. Lett. **21**, 617 (1968).
[14] K. Adachi, M. Matsui, and M. Kawai, J. Phys. Soc. Jpn. **46**, 1474 (1979).
[15] S. Ogawa and T. Yamadaya, Phys. Lett. A **47**, 213 (1974).
[16] A. Ohsawa, Y. Yamaguchi, H. Watanabe, and H. Itoh, J. Phys. Soc. Jpn. **40**, 986 (1976).
[17] H. Hiraka, Y. Endoh, and K. Yamada, J. Phys. Soc. Jpn. **66**, 818 (1997).
[18] S. Yomo, J. Phys. Soc. Jpn. **47**, 1486 (1979).
[19] H. Hiraka and Y. Endoh, J. Phys. Soc. Jpn. **65**, 3740 (1996).
[20] T. Goto, Y. Shindo, H. Takahashi, and S. Ogawa, Phys. Rev. B **56**, 14019 (1997).
[21] S. Barakat, D. Braithwaite, P. Alireza, K. Grube, M. Uhlarz, J. Wilson, C. Peiderer, J. Flouquet, and G. Lonzarich, Phys. B (Amsterdam, Neth.) **359-361**, 1216 (2005).
[22] V. A. Sidorov, V. N. Krasnorussky, A. E. Petrova, A. N. Utyuzh, W. M. Yuhasz, T. A. Lograsso, J. D. Thompson, and S. M. Stishov, Phys. Rev. B **83**, 060412(R) (2011).
[23] P. Ohresser, E. Otero, F. Choueikani, K. Chen, S. Stanescu, F. Deschamps, T. Moreno, F. Polack, B. Lagarde, J. P. Daguerre *et al.*, Rev. Sci. Instrum. **85**, 013106 (2014).
[24] F. Baudelet, L. Nataf, and R. Torchio, High Pressure Res. **36**, 429-444 (2016).
[25] M. Benfatto, A. Congiu-Castellano, A. Daneile, and S. D. Longa, J. Synchrotron Radiat. **8**, 267 (2001).
[26] V. V. Brazhkin, L. N. Dzhavadov, and F. S. El'kin, JETP Lett. **104**, 99 (2016).
[27] H. Miyauchi, T. Koide, T. Shibara, N. Nakajima, H. Kawabe, K. Yamaguchi, A. Fujimori, H. Fukutani, K. Iio, and T. Miyadai, J. Electron Spectrosc. Relat. Phenom. **78**, 255 (1996).
[28] T. Muro, T. Shishidou, F. Oda, T. Fukawa, H. Yamada, A. Kimura, S. Imada, S. Suga, S. Y. Park, T. Miyahara, and K. Sato, Phys. Rev. B **53**, 7055 (1996).
[29] V. N. Antonov, O. V. Andryushchenko, A. P. Shpak, A. N. Yaresko, and O. Jepsen, Phys. Rev. B **78**, 094409 (2008).
[30] G. van der Laan and B. T. Thole, Phys. Rev. Lett. **60**, 1977 (1988).
[31] C. T. Chen, Y. U. Idzerda, H.-J. Lin, N. V. Smith, G. Meigs, E. Chaban, G. H. Ho, E. Pellegrin, and F. Sette, Phys. Rev. Lett. **75**, 152 (1995).
[32] C. Brouder and M. Hikam, Phys. Rev. B **43**, 3809 (1991).
[33] J.-i. Igarashi and K. Hirai, Phys. Rev. B **53**, 6442 (1996).
[34] A. L. Ankudinov and J. J. Rehr, Phys. Rev. B **56**, R1712(R) (1997).
[35] V. N. Antonov, B. N. Harmon, and A. N. Yaresko, Phys. Rev. B **67**, 024417 (2003).
[36] C. R. Natoli, in *EXAFS and Near Edge Structure*, edited by A. Bianconi, L. Incoccia, and S. Stipcich, Springer Series in Chemistry and Physics, Vol. 27 (Springer, Berlin, 1983), p. 43.
[37] X. B. Liu and Z. Altounian, J. Appl. Phys. **101**, 09G511 (2007).
[38] A. Y. Ramos, C. Piamonteze, H. C. N. Tolentino, N. M. Souza-Neto, O. Bunau, Y. Joly, S. Grenier, J.-P. Itié, N. E. Massa, J. A. Alonso, and M. J. Martinez-Lope, Phys. Rev. B **85**, 045102 (2012).
[39] A. Y. Ramos, N. M. Souza-Neto, H. C. N. Tolentino, O. Bunau, Y. Joly, S. Grenier, J.-P. Itie, A.-M. Flank, P. Lagarde, and A. Caneiro, Europhys. Lett. **96**, 36002 (2011).

Correction: The author name Y. Mijiti has been changed to E. Mijit.